Ferrocenoyl Derivatives of Alamethicin: Redox-Sensitive Ion Channels†

Jeffrey D. Schmitt,‡ M. S. P. Sansom,§ I. D. Kerr,§ G. G. Lunt,‡ and R. Eisenthal*,‡

School of Biology and Biochemistry, University of Bath, Claverton Down, Bath BA2 3AY, U.K., and Laboratory of Molecular Biophysics, University of Oxford, Rex Richards Building, South Parks Road, Oxford OX1 3QU, U.K.

Received August 26, 1996; Revised Manuscript Received November 11, 1996⊗

ABSTRACT: The synthesis and single-channel characterization of two redox-active C-terminal derivatives of alamethicin are herein described. The reduced [Fe(II)] forms of ferrocenoyl-alamethicin (Fc-ALM) and 1′-carboxyferrocenoyl-alamethicin (cFc-ALM) are shown to form voltage-dependent ion channels at *cis* positive potentials in planar lipid bilayers (PLB) with conductance properties similar to those of alamethicin. *In situ* oxidation of Fc-ALM [to Fe(III)] in the PLB apparatus causes a time-dependent elimination of channel openings, which can be restored by an increase in the transbilayer potential. In contrast, oxidation of cFc-ALM leads to the formation of shorter-lived channels. Pretreatment of the ferrocenoyl peptides with oxidizing agent alters their single-channel properties in a qualitatively similar manner, establishing that the changes in channel properties in the presence of oxidizing agents are due specifically to ferrocenoyl oxidation. We suggest that the redox sensitivity of these ferrocene-containing ion channels may be governed by a combination of the following factors: (1) changes in hydrophobicity; (2) alteration of peptide molecular dipole; and (3) alterations in tendencies toward self-association. However, oxidation induced changes in peptide conformation cannot be ruled out. Our results provide evidence that it is possible to engineer channel-forming peptides that respond to specific changes in the chemical environment.

Alamethicin is perhaps the best-characterized member of the family of channel-forming peptides (CFPs)[1] known as peptaibols (Woolley & Wallace, 1993; Sansom, 1993a; Latorre & Alvarez, 1981). Alamethicin self-associates in lipid bilayers in a voltage-dependent fashion to form ion channels. Significant evidence has accumulated that supports the "barrel-stave" model of ion channel formation, whereby α-helical monomers of the peptide insert into the bilayer and aggregate to form bundles (Baumann & Mueller, 1974; Boheim, 1974), thus creating a pore through which ions can pass (Sansom, 1993b). These bundle-like assemblies are of mounting interest since they may be prototypical of biologically important ligand gated ion channels such as the nicotinic acetylcholine receptor (Karlin & Akabas, 1995; Unwin, 1993). Moreover, the size of the assemblies is well within the limits of computational simulation. There is also an ever increasing interest in channel peptides with novel properties for potential use in biosensor technology and nanodevices (for a review, see: Schnur & Peckerar, 1992).

Two recent reports by Woolley and co-workers demonstrate that it is possible to alter significantly the biophysical properties of alamethicin through C-terminus modification. In the first report the pyromellitoyl ester of alamethicin is shown to form channels with significantly higher single-channel conductance levels, longer open times, and a markedly increased sensitivity to divalent ions compared to alamethicin itself (Woolley et al., 1994). These investigators also show that in macroscopic measurements higher transbilayer potentials are required for channel activation. Their most recent report demonstrates that tethering alamethicin monomers together using flexible covalent linkages leads to the formation of ion channels with markedly increased conductance lifetimes and a significantly narrower distribution of assembly sizes (You et al., 1996).

On a related front, DeGrado's group (DeGrado & Lear, 1990; Akerfeldt, 1993) have demonstrated that helical peptides with very simple amino acid composition, i.e., leucine and serine, can form voltage-gated ion channels similar to alamethicin and other channel-forming peptides. Similar peptides have been constructed from leucine and lysine (Cornut et al., 1994). The nonhelical cyclic peptide "nanotubes" designed by Ghadiri and co-workers (Ghadiri et al., 1993, 1994) have also been shown to form ion-selective channels, thus leading to new possibilities in the design of molecular devices.

As part of a related effort, we have been motivated to create CFPs with sensitivity to their chemical environment. We now report our results of our investigations with alamethicin esterified with fecerrocenecarboxylic acid or 1,1′-ferrocenedicarboxylic acid (Figure 1A). The redox-active metallocene bis(cyclopentadienyl)iron, or ferrocene, was chosen because of its unique redox properties (Figure 1B): the iron center can be easily oxidized and reduced chemically or electrochemically. In addition, the oxidized (blue) form

†This work was supported by a grant from the Molecular Electronics Initiative of the Engineering and Physical Sciences Research Council of England (Grant GR-J02964) and by an Overseas Research Studentship and University of Bath Studentship (J.D.S.), and by a grant from the Wellcome Trust (M.S.P.S.).

‡ University of Bath.

§ University of Oxford.

⊗ Abstract published in *Advance ACS Abstracts,* January 1, 1997.

[1] Abbreviations: ALM, alamethicin; BES, *N*,*N*-bis(2-hydroxyethyl)-2-aminoethanesulfonic acid; CAN, cerium(IV) ammonium nitrate; cFc-ALM, 1′-carboxyferrocenoyl-alamethicin; CFP, channel-forming peptide; DPhPC, diphytanoylphosphatidylcholine; DMAP, 4-(*N*,*N*-dimethylamino)pyridine; DMF, dimethylformamide; Fc-ALM; ferrocenoyl-alamethicin; HOAc, acetic acid; LDMS, laser desorption mass spectrometry; HPLC, high pressure liquid chromatography; MeCN, acetonitrile; MeOH, methyl alcohol; F′, phenolalaninol; R_f, TLC retentivity factor; V_t, potential required to elicit a 100 pA current in macroscopic current−voltage measurements.

S0006-2960(96)02168-X CCC: $14.00

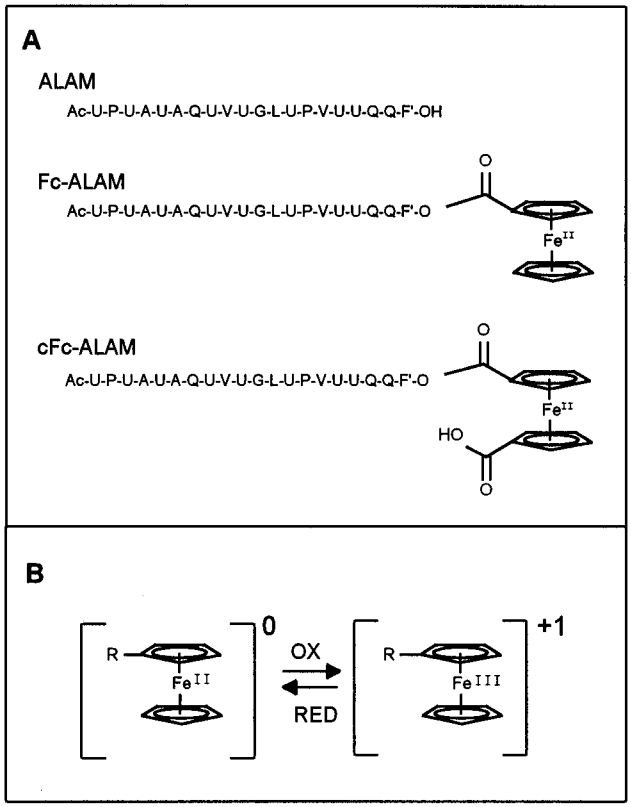

FIGURE 1: (A) Chemical structures of $R_f = 50$ alamethicin (ALM), ferrecenoyl-alamethicin (Fc-ALM), and 1′-carboxyferrocenoyl-alamethicin (cFc-ALM). Standard single letter abbreviations for amino acids are used; Ac is acetate, U, α-aminoisobutyric acid (Sansom, 1993); and F′, phenylalaninol. (B) Reduced Fe(II) and oxidized Fe(III) states of ferrocene.

of ferrocene is diamagnetic whereas the reduced (orange) form is not.

Thus, the introduction of a dual chromophoric and magnetophoric moiety into the peptide offers new possibilities through which to probe the behavior of CFPs. Fc-ALM and cFc-ALM show modified channel-forming properties relative to the parent peptide. Moreover, the channel activity of the two ferrocenoyl derivatives is sensitive to their redox state. These changes are discussed in terms of possible molecular mechanisms of channel formation. Finally, we present evidence for a mechanism that may contribute to the redox sensitivity of channels formed from these peptides.

MATERIALS AND METHODS

Ferrocenecarboxylic acid, 1,1′-ferrocenedicarboxylic acid, 4-(*N*,*N*-dimethylamino)pyridine, sodium dithionite, and cerium(IV) ammonium nitrate were purchased from Aldrich Chemical Co. (Poole, U.K.). High purity *N*,*N*-bis(2-hydroxyethyl)-2-aminoethanesulfonic acid and the $R_f = 50$ molecular species of alamethicin from *Trichoderma viride* were purchased from Sigma Chemical Co. (Poole, U.K.). Diphytanoylphosphatidylcholine was purchased from Avanti Polar Lipids (Alabaster, AL). Sephadex LH-20 was purchased from Pharmacia Biotech (Uppsala, Sweden). Pyridine was dried by distillation from calcium hydride; dimethyl formamide was distilled over dried 4 Å molecular sieves prior to use. Water used in peptide purification and PLB work was double distilled and further purified using a Milli-Q purification system. Ferrocenoic anhydride was synthesized according to the method of Acton and Silverstein (1955).

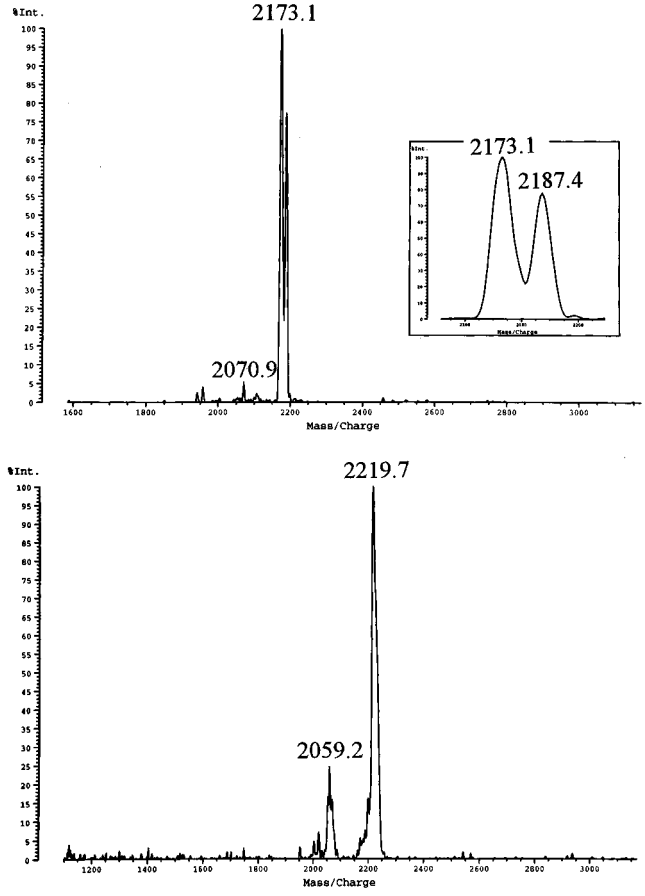

FIGURE 2: Mass spectral results. Samples were dissolved in 200 μL of methanol, and a small portion (<1 μL) was applied to a sample slide, dried, and then overlaid with 1 μL of matrix solution (10 mg/mL α-cyano-4-hydroxycinnamic acid (panel A) or 10 mg/mL sinapinic acid (panel B) in 50% acetonitrile/0.1% trifluoroacetic acid). The dried sample spot was then washed with high grade water (2 × 5 μL) and then dried again before placing the slide in the mass spectrometer. Spectra were recorded on a Kratos MALDI III mass spectrometer in linear mode with negative ionization at threshold laser power and 20 kV accelerating voltage. Calibration was internal with 1 pmol/μL oxidized insulin B chain. If necessary, serial dilutions of the original sample in methanol were examined to obtain the best signal to noise response. Fc-ALM (top trace) expected mass: 2187.0 ($[M - H]^-$); observed mass: 2187.4 ($[M - H]^-$) , 2173.1 ($[M - H_2O]^-$), 2070.9 ($[M - FeC_5H_5]^-$). cFc-ALM (bottom trace) expected mass: 2219.0 ($[M - H]^-$) ; observed mass: 2219.7 ($[M - H]^-$), 2059.2 ($[M - FeC_5H_5COOH]^-$).

Ferrocene-1,1′-dicarboxylic acid dichloride was prepared by the method that Lau and Hart (1958) used for the preparation of ferrocenoyl chloride with appropriate stoichiometric modifications (data not shown) and recrystallized from petroleum ether (bp 60−80 °C) as dark red crystals. Sep-Pak C_{18} reverse phase chromatography cartridges were purchased from Waters Ltd. (Watford, U.K.). Glass thin-layer chromatography (TLC) plates were purchased from Whatman Inc. (Maidstone, U.K.). TLC plates were developed in one of the following systems: system A ($CHCl_3$/MeOH/H_2O, 65:25:2 v/v) or system B ($CHCl_3$/MeOH/H_2O/HOAc, 70:30:3:2 v/v). After development, spots were visualized by Cl-tolidine reagent (Stahl, 1965). Details of mass spectrometric analysis are given in the legend of Figure 2.

Synthesis of Ferrocenoyl-alamethicin. The following synthesis is based on an adaptation of the published method of Woolley et al. (1994). Alamethicin (7.5 mg, 3.6 μmol),

DMAP (10 mg, 82 μmol), and ferrocenoic anhydride (125 mg, 264 μmol) were dissolved in 1.2 mL of dry DMF and 0.5 mL of pyridine. The mixture was stirred overnight under a nitrogen atmosphere. The reaction was quenched by the addition of 1.8 mL of distilled water in small portions. After stirring for a short period, a precipitate formed which was removed by centrifugation. The entire reaction mixture was applied to an LH-20 gel filtration column (2 × 30 cm), eluted with methanol at a flow rate of 10 mL/min, and monitored for absorbence at 260 nm. The first peak to elute was collected and solvents were removed by rotary evaporation. The residue was dissolved in MeCN and loaded onto a Sep-Pak cartridge. The cartridge was then washed with 5 mL of water, followed by elution of peptide with 15 mL of MeCN. The eluent was dried and the above process repeated. The resulting residue was dissolved in acetonitrile and purified by reverse phase HPLC (Zorbax C_{18}, using a linear gradient of H_2O/MeCN, starting at 91:9 H_2O/MeCN and ending at 10:90 H_2O/MeCN). Using a flow rate of 2.0 mL/min, the desired product eluted at 95 min. The product migrates as one spot on TLC using system A, $R_f = 0.7$, compared to alamethicin $R_f = 0.4$. negative ion LDMS: 2187.4 ([M − H]$^-$), 2173.1 ([M − H_2O]$^-$), 2070.9 ([M − FeC_5H_5]$^-$), Figure 2 (top trace).

Synthesis of 1′-Carboxyferrocenoyl-alamethicin. During the course of our investigations, a simpler method for the synthesis and purification of the peptides was developed and used to make the following compound. Ferrocene-1,1′-dicarboxylic acid dichloride (100 mg, 321.7 μmol) and alamethicin (10 mg, 4.8 μmols, stored *in vacuo* over phosphorus pentoxide) were combined in a flame-dried screw-capped tube (Teflon septum) with a stirring bar, followed by the addition of 1 mL of dry pyridine. The reaction mixture was vigorously stirred under argon for 36 h, at which time only a trace of starting material remained. The reaction was quenched with 0.5 mL of water and stirred for an additional 4 h. To reduce any ferrocenic compounds that may have oxidized during the course of the reaction, 0.2 mL of concentrated aqueous sodium dithionite was added. The solvents were removed under a stream of nitrogen followed by *in vacuo* removal of any remaining volatiles. The mixture was suspended in 1−2 mL of methanol and applied to a Sephadex LH-20 column (2 × 30 cm) equilibrated in methanol. Products were eluted with methanol (acidified with 1% HOAc, gravity flow ∼5 mL/min), taking 2 mL fractions. The peptide-containing fractions were pooled, concentrated, and reapplied to an LH-20 column (1.5 × 20 cm) and eluted with the same solvent (gravity flow ∼4 mL/min), collecting 1 mL fractions. The desired product eluted as a single band having an $R_f = 0.3$, compared to alamethicin $R_f = 0.45$, in TLC system B. Negative ion LDMS: 2219.7 ([M − H]$^-$), 2059.2 ([M − FeC_5H_4COOH]$^-$), Figure 2 (bottom trace). Pyridine was found to have a deleterious effect on chromatographic separation of the peptides using LH-20.

Planar Lipid Membrane Experiments. The method of Montal and Mueller (1972) was used to form planar DPhPC bilayers across an approximately 100 μm perforation in a 25 μm thick Teflon membrane (for a review of the methodology, see Hanke & Schule, 1993). Briefly, DPhPC monolayers were formed between two electrolyte-filled chambers separated by a Teflon membrane in which a spark-polished hole has been formed. After priming the hole with hexadecane, the electrolyte level (buffered KCl) of the chambers is simultaneously raised in such a way that the monolayers fold together at the hole and form a stable bilayer. Measurements were performed using silver/silver chloride electrodes and an Axopatch (CV-9B) head-stage amplifier, Axopatch Patch-Clamp D-1 amplifier, Digidata AD converter, and Axoscope Data analysis software (Axon Instruments, Foster City, CA). Data were recorded directly to hard disk after filtering with an 8-pole Bessel filter at 5 kHz, unless otherwise indicated. Aliquots of ALM, Fc-ALM, or cFc-ALM were added to the *cis* side of the bilayer as methanolic solutions, unless otherwise indicated. Likewise, requisite amounts of oxidizing agents were taken from freshly made solutions. By convention, the potential in the *cis* chamber of the PLB apparatus is defined relative to the *trans* chamber which is grounded (i.e., $V = 0$ mV). A positive current indicates positive ion flow from the *cis* to the *trans* chamber of the apparatus. Experiment specific details are given in the figure legends.

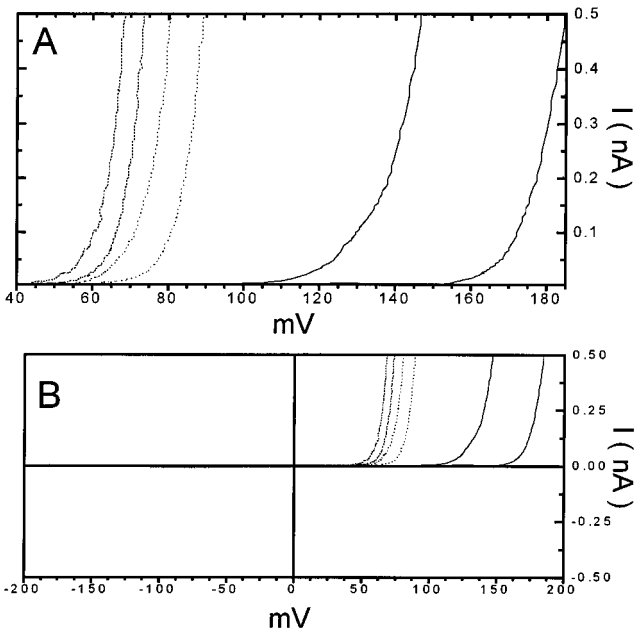

FIGURE 3: Current−voltage ($I-V$) measurements in planar lipid bilayers. Peptides were added to the *cis* (positive potential) chamber of the PLB apparatus to a final concentration of 0.25 μM in buffered electrolyte (0.5 M KCl, 10 mM BES, pH 7.0). Triangular voltage sweeps ($\lambda = 20$ s) from −100 to +100 mV for ALM, −90 to +90 mV for Fc-ALM, and −180 to +180 mV for cFc-ALM were then applied. Currents from 20 such sweeps were averaged together and are plotted as follows: ALM (···); Fc-ALM (- - -); and cFc-ALM (—). The right hand curve of each pair represents the induced current during the ascending portion of the voltage sweep (i.e., dV/dt > 0) and the left hand curve the descending (dV/dt < 0) portion. Note the marked hysteresis with cFc-ALM (panel A). Full scale $I-V$ curve (panel B) shows the asymmetry of channel activation in all three peptides.

RESULTS

Synthesis of Alamethicin Derivatives. Two ferrocene ester derivatives of alamethicin were synthesized: ferrocenoyl-alamethacin and 1′-carboxyferrocenoyl-alamethacin (Figure 1). Synthesis and purification of ferrocenoyl-alamethicin were achieved by adaptation of the method for synthesis of alamethicin pyromellitate (Woolley et al., 1994). Synthesis of 1′-carboxyferrocenoyl-alamethicin proceeded smoothly by reaction of the anhydrous alamethicin with ferrocene-1,1′-

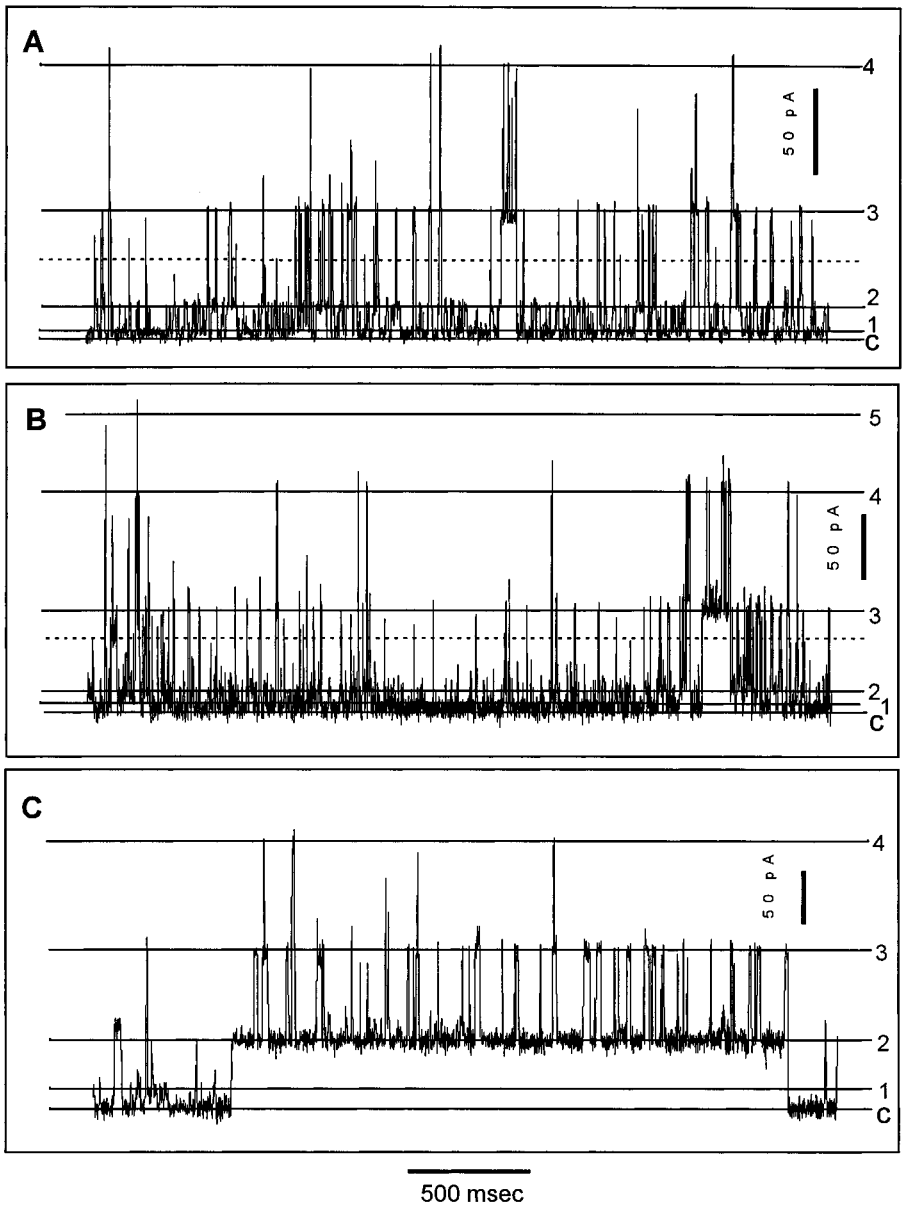

FIGURE 4: Three seconds of single-channel recording from 0.375 μM ALM (panel A), 0.25 μM Fc-ALM (panel B), and 0.25 μM cFc-ALM (panel C). Peptides were added to the *cis* chamber of the PLB apparatus; each chamber contains 2 mL of buffered electrolyte (0.5 M KCl, 10 mM BES, pH 7.0). The following potentials were applied: +140 mV, panel A; +170 mV, panel B; +136 mV, panel C.

dicarboxylic acid dichloride in pyridine followed by hydrolysis of the remaining acid chloride (*N*-acylpyridinium salts) with water. During the course of the investigations, a significantly simpler purification method was devised. Both the HPLC purification and the Sephadex LH-20 based purification methods yielded one product, as evidenced by TLC and mass spectrometry (Figure 2). We found no evidence for contamination of either peptide with unmodified alamethicin.

Planar Lipid Bilayer Studies. To evaluate the channel-forming behavior of these peptides, we conducted both macroscopic current−voltage and single-channel measurements using planar lipid bilayers. When Fc-ALM and cFc-ALM are incorporated into diphyantoylphosphatidylcholine PLBs, they form voltage-sensitive channels similar to alamethicin. Figure 3 demonstrates that higher potentials are required to activate equivalent concentrations of the ferrocene-containing peptides. This can be shown by measuring the voltage, V_t, required to elicit a 0.1 nA current. V_t values for Fc-ALM and cFc-ALM are +81 and +174 mV, respectively, compared to +66 mV for ALM. These peptides only form channels at *cis* positive potentials, consistent with the behavior of native alamethicin (Figure 3B). This figure demonstrates a marked increase in hysteresis of the current−voltage relationship of cFc-ALM compared to Fc-ALM or ALM. Hysteresis is reflected in the difference between induced current during ascending and descending portions of the voltage sweep.

The single-channel properties of these peptides also appear similar to those of alamethicin. Figure 4 indicates that, despite the need for higher activation potentials, the ferrocenoyl ALM channels (Figure 4B) are qualitatively comparable to ALM. The cFc-ALM channels exhibit more complex gating kinetics than do the other peptides; there appear to be two distinct populations, the first having lifetimes of approximately 500−3000 ms and an additional group having 10−50 ms lifetimes (Figure 4C). Note that the short lifetime openings appear more frequently when the channel is already open to the 2nd conductance level. Gaussian curves were fit to the single-channel conductance

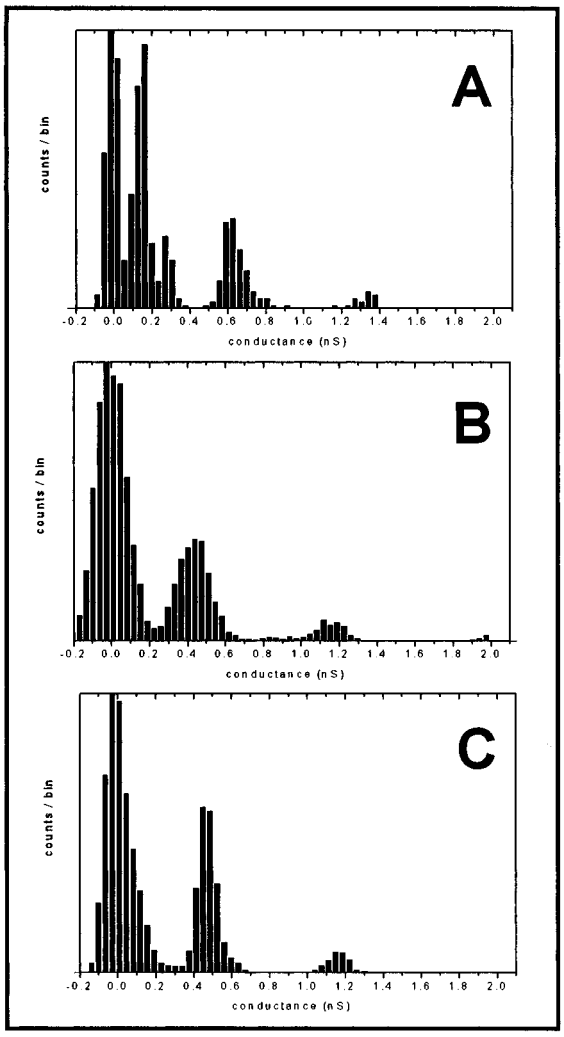

FIGURE 5: Single-channel conductance histograms for ALM, panel A; Fc-ALM, panel B; and cFc-ALM, panel C. Experimental details are given in the legend of Figure 4.

Table 1: Conductance Levels of Peptides: Including Reduced and Oxidized Forms of Fc-ALM and cFc-ALM[a]

	conductance (nS)				
level	ALM	Fc-ALM	Fc-ALM(ox)	cFc-ALM	cFc-ALM(ox)
1	0.14[b]	0.15[b]	0.10	0.11[b]	0.11[b]
2	0.28	0.24[b]			0.37
3	0.62	0.43	0.52	0.46	0.68
4	1.34	1.15		1.16	0.84
5		1.75[b]		1.70[b]	0.99
6					1.14[b]
7					2.03[b]

[a] Levels were calculated by fitting conductance histograms with multiple Gaussian curves. [b] Indicates manual measurement.

histograms for ALM, Fc-ALM, and cFc-ALM shown in Figure 5. The results of the single-channel subconductance levels are summarized in Table 1.

The effect of oxidative conditions on channel formation was explored using two approaches, employing the oxidizing agent cerium ammonium nitrate. In the first experiments, excess CAN was added directly to the *cis* side of the PLB apparatus during single-channel recording. In subsequent experiments, the ferrocenoyl peptides were combined with buffered CAN before addition to the PLB apparatus.

The *in situ* addition of CAN causes a time-dependent diminution of Fc-ALM channels at constant bilayer potential;

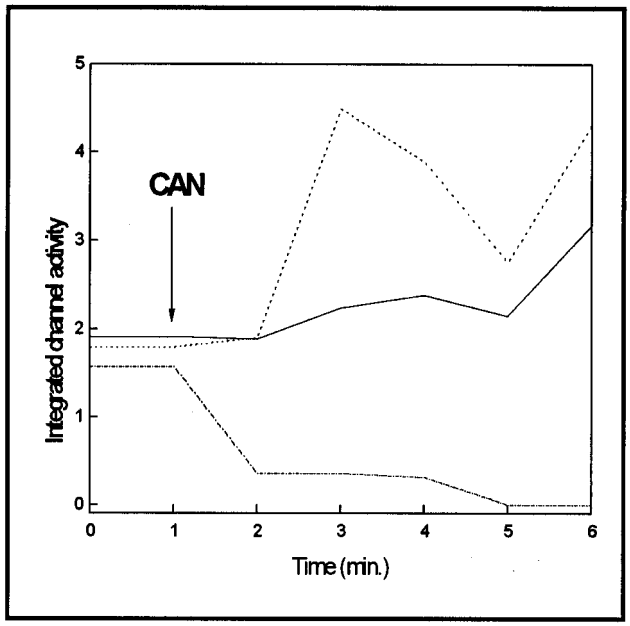

FIGURE 6: Average channel activity levels from ALM (—), Fc-ALM (—•—), and cFc-ALM (- - -), in the presence of 2.5 mg/mL CAN. Peptides were added to the *cis* chamber of the PLB apparatus to a final concentration of 0.25 μM; each chamber contains 2 mL of buffered electrolyte (0.5 M KCl, 10 mM BES, pH 7.0). Single-channel traces were divided into 1 min sections, and the total peak area for each section was calculated by integration. Data points are normalized to match the signal level of ALM before the addition of CAN. The zero time point was derived from 1 min of channel recording before the addition of CAN (indicated by arrow).

in the case of cFc-ALM, the long lifetime openings appear to be selectively eliminated. CAN appears to not to exhibit these effects on alamethicin channels, as shown in Figure 6. Note that channel activity of the oxidized Fc-ALM peptides can be restored by increasing the bilayer potential by 25−35 mV (data not shown). Furthermore, with ALM and other CFPs, one observes an increase in net channel conductance during the course of $I-V$ experiments. The presence of CAN alleviates this temporal current increase in Fc-ALM and cFc-ALM but not ALM, additional evidence that oxidative conditions elicit a specific effect on the ferrocenoyl peptides (data not shown).

Premixing of peptide and CAN produced similar results. Figure 7 shows representative traces of Fc-ALM (panel A) and cFc-ALM (panel B) pretreated with CAN. Note that two separate sections of a channel recording are shown side-by-side in panel A due to sparseness of Fc-ALM channel activity. In both cases, the final concentration of peptide added to the PLB apparatus was about twice that required to elicit channel activity by the corresponding peptide in the absence of CAN (see figure legend). Conductance histograms shown in (Figure 8) suggest that the oxidized peptides mainly open to the first one or two conductance levels, in contrast to the reduced peptides (Figure 5), and that the percentage of time spent in the closed state is greater for the oxidized peptides. Table 1 also summarizes the results of multiple Gaussian fittings to these histograms, although these results may be somewhat inaccurate due to short opening times.

DISCUSSION

Based on the finding of Woolley and co-workers (1994) that the C-terminus pyromellitoyl ester of alamethicin acts

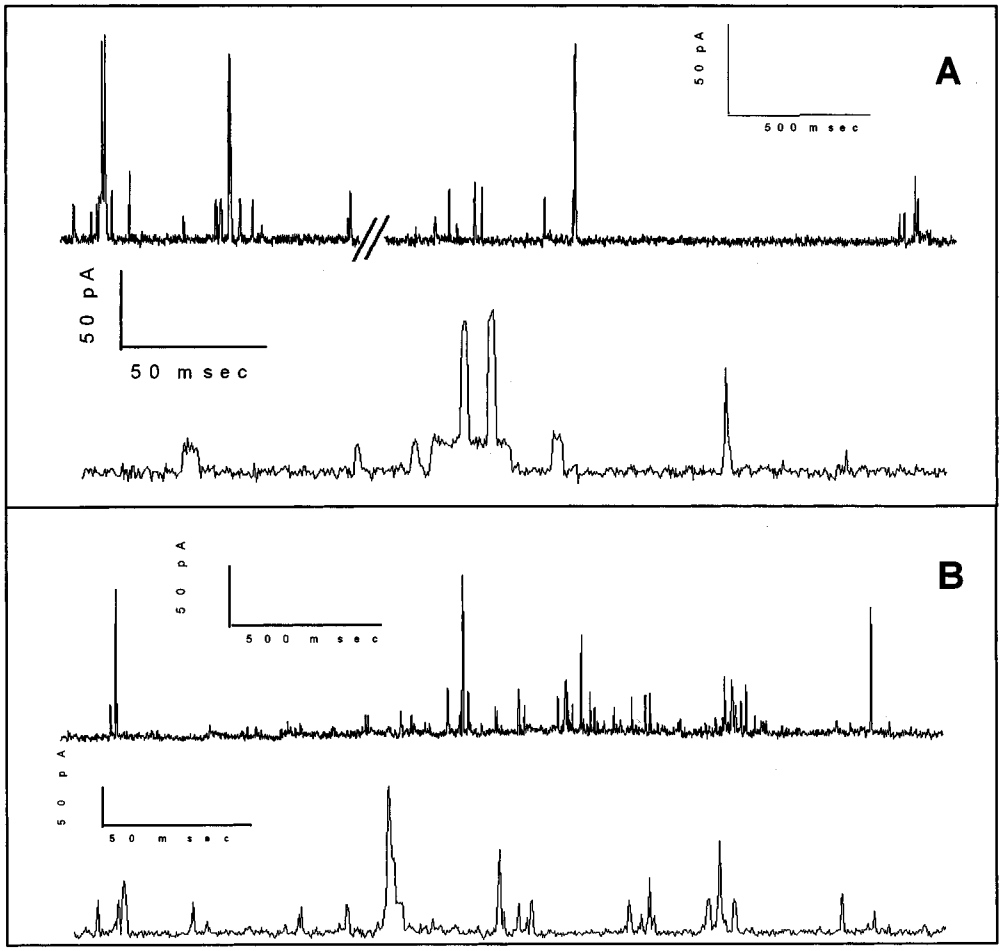

FIGURE 7: Single-channel recordings from 0.5 μM Fc-ALM (panel A) and 0.5 μM cFc-ALM (panel B) premixed for 3 min with 20 μL of 10 mM CAN and 20 μL of electrolyte buffer. This quantity of CAN is 10-fold the molar ratio required to fully oxidize the either ferrocenecarboxylic acid or ferrocenedicarboxylic acid in 3 min (determined by spectrophotometric titration, data not shown). Peptides were added to the *cis* chamber of the PLB apparatus; each chamber contains 2 mL. of buffered electrolyte (0.5 M KCl, 10 mM BES, pH 7.0). The following potentials were applied: +185 mV, panel A; and +96 mV, panel B. Data in each case are displayed on two different time scales.

as a "calcium-activated channel forming peptide", we synthesized two ferrocenoyl alamethicin esters and evaluated their behavior under neutral and oxidative conditions. Our postulate that CFPs with redox sensitivity could be designed has been validated by the experiments described. We interpret these data based on the "barrel-stave" model of channel formation and thus consider possible effects on membrane association (dependent on hydrophobicity), orientation of the bound peptide relative to the bilayer (related to the net molecular dipole of the peptide helix), and self-association of the peptide within the bilayer.

Macroscopic current−voltage measurements indicate that both the ferrocenoyl and 1′-carboxyferrocenoyl peptides require a higher transbilayer potential to induce channel formation (V_t) relative to the parent peptide (Figure 2). Since Fc-ALM is uncharged in the reduced state, we attribute this to steric and/or conformational effects imposed by the bulky ligand and to a decrease in the net molecular dipole. In the case of cFc-ALM, the introduction of a negatively charged carboxyferrocene ester (1,1′- dicarboxyferrocene monoethyl ester, pK_a = 6.08 (measured in 68% MeOH (aq) (Nesmeyanov & Reutov, 1957), this value may be as low as 5.0 if extrapolated to 100% H_2O) causes a further increase in V_t; this finding is qualitatively consistent with the effect observed by Woolley and co-workers (1994) where addition of a $(\text{pyromellitoyl})^{3-}$ ester roughly triples V_t. On the other hand, it is likely that additional steric or conformational effects contribute to the behavior of cFc-ALM: introduction of the carboxyferrocene, with its single negative charge, also triples its activation potential relative to ALM. The relationship between Fc-ALM and cFc-ALM is consistent with the observation of Hall et al. (1984) that (Glu19-benzoyl) R_f = 30 ALM has a lower V_t than R_f = 30 ALM. Overall, it is clear that C-terminus modification of ALM leads to higher activation potentials. It is important to note that cFc-ALM also exhibits markedly higher hysteresis compared to ALM or Fc-ALM (Figure 3A). It is possible that the carboxylate ion forms stabilizing *inter*molecular interactions once the channels assemble, leading to hysteresis. However, similar effects are not seen with pyromellitoyl-alamethicin, as one would expect based on this argument (Woolley, personal communication).

The single-channel conductance levels of Fc-ALM are slightly lower than those of alamethicin (Table 1). Possible explanations include the effect of added steric bulk at the mouth of the channel or favorable aromatic−cation interactions supported by the ferrocenoyl moieties which may hinder the free passage of ions through the channels. It also appears that the opening times are shorter (Figure 4). The conductance levels for cFc-ALM are nearly identical to those of Fc-ALM, although the presence of the carboxylate ion in the former increases the conductance levels slightly (Table

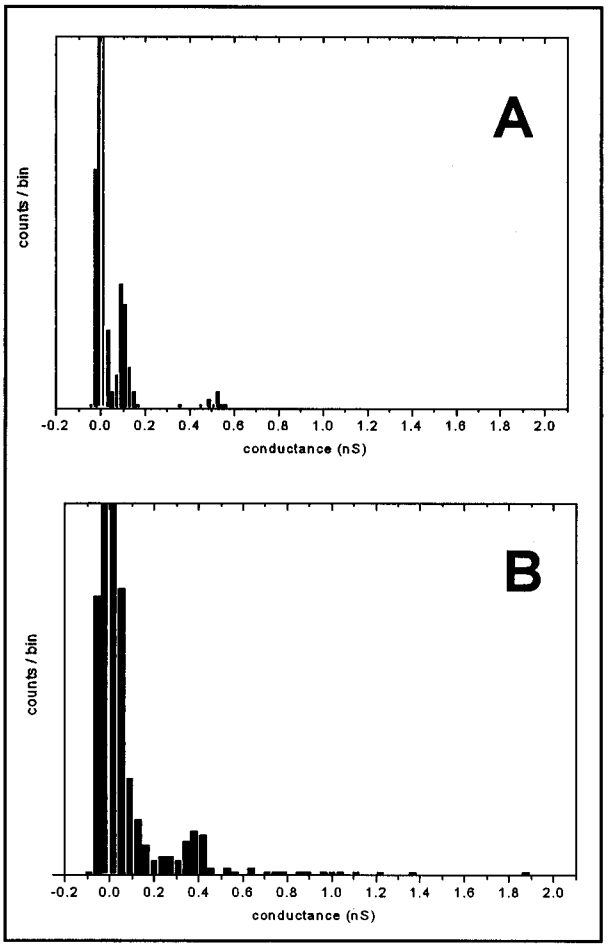

FIGURE 8: Single-channel conductance histograms from the CAN premixing experiments described in the legend of Figure 7: Fc-ALM, panel A; and cFc-ALM, panel B.

1). However, the temporal behavior of the cFc-ALM channels is dramatically different from either ALM or Fc-ALM (Figure 4C), single-channel traces characterized by long opening times. Unlike the other peptides, one aggregation state (the $n = 2$ level) of cFc-ALM seems particularly stable, as evidenced by the population of long-lived channels at $n = 2$. Short-lived bursts to higher conductance levels ($n = 3, 4$) appear frequently during these long-opening events. One is compelled to reason that these bursts represent short sojourns to substates of the long-lived channels since the short-lived bursts occur less frequently in the absence of the stable population. However, the possibility that these conductance bursts represent multiple openings cannot be ruled out.

The *in situ* addition of cerium ammonium nitrate to Fc-ALM channels causes the elimination of single-channel activity at a given holding potential, an effect not seen with ALM channels. Calculations indicate that the orientation of the net molecular dipole of Fc-ALM may reverse upon oxidation (Table 1). Channel activity can however be restored by increasing the bilayer potential 25−35 mV (data not shown). Again, this is consistent with the finding that the presence of charged groups at the termini of CFPs decrease their propensity to form channels. Figure 7 compares the behavior of ALM, Fc-ALM, and cFc-ALM channels under oxidative conditions; it appears that the introduction of a positive charge counterbalances the deleterious effect of the carboxylate ion in cFc-ALM; i.e., oxidation of Fc-ALM results in a charged C-terminus, but oxidation of cFc-ALM results in a neutral C-terminus. Thus three types of redox behavior are evident: (1) oxidative conditions elicit no effect [ALM], (2) decrease channel activity [Fc-ALM], and (3) increase channel activity [cFc-ALM].

Table 2: Comparision of V_t, Hydrophobicity (F_{oct}), Charge, and Molecular Dipole[a]

peptide	V_t (mV)	F_{oct} (kcal/mol)[c]	charge	molecular dipole (D)[b] moment	*z*-component
ALM	66	−117.5	0	81.3	76.4
Fc-ALM	81	−116.7	0	25.5	22.5
Fc-ALM(ox)	>200	−113.9	+1	32.6	−31.2
cFc-ALM	174	−115.4	−1	84.6	75.4
cFc-ALM(ox)	<170	−112.6	0	43.5	27.8
ALM-pm	198	−111.1	−3	369.8	366.1

[a] The values listed above are quantitative estimates. ALM-pm: pyromellatoyl alamethicin (Woolley et al., 1994). [b] Calculated using charge equilibration derived charges, as described by Rappé and Goddard (1991); peptides were modeled in helical form and aligned with the helical axis in the *z*-direction and the C-terminus at the coordinate origin. [c] Calculated free energy in octanol relative to vacuum, as described by Pearlman (1980), with added parameters for ferrocene: −0.570 for the reduced form and 0.840 for the oxidized form.

It might be argued that the large concentration of CAN present in the *in situ* experiments was eliciting a nonspecific effect. To address this possibility, small quantities of peptides and buffered CAN were combined prior to addition to the PLB apparatus. Single-channel traces clearly indicate that these conditions alter the characteristics of both Fc-ALM and cFc-ALM channels (Table 1; compare Figures 4B to 7A and 4C to 7B). Opening lifetimes are considerably shorter, and in the case of Fc-ALM the highest observed conductance state is absent. This is in marked contrast to cFc-ALM where one favored conductance state is replaced by a number of equally probable levels; indeed the long openings observed with reduced cFc-ALM appear to be selectively eliminated by oxidation of the ferrocenoyl moiety. The possibility that the cerium ions are participating in specific interactions such as coordination by the aromatic-rich C-termini of the channels cannot be ruled out. It is also somewhat suprising that Fc-ALM does not form channels at *cis* negative potentials given the hydrophobic nature of the reduced ferrocene moiety.

Although our results are consistent with the concept that channel formation is modulated by a combination of well established factors, such as peptide hydrophobicity and alignment of the molecular dipole against the imposed field, it is not feasible at present to quantify the extent to which each of these factors contributes to the behavior of the ferrocenoyl peptides. Estimates of hydrophobicity, molecular dipole, and charge relative to ALM are given in Table 2. It is also possible that the introduction of charge may create disfavored electrostatic interactions with the phosphocholine headgroups. This view is consistent with the observation that introduction of negative charge into the C-terminus in pyromellitoyl peptide increases its conductance threshold (Woolley et al., 1994). One might also speculate that attractive cation−aromatic interactions between F′-20 and the Fe(III) center may induce conformational changes in the oxidized peptides relative to the reduced. Favorable cation−aromatic interaction has been postulated to be important in

a number of systems (Dougherty & Stauffer, 1990). In addition, the *cis* lumen of the ferrocenoyl channels is very rich in aromatic character due to the presence of multiple F′ side chains and ferrocene moieties, possibly giving rise to enhanced interaction with solvated ions.

We have provided evidence that Fc-ALM and cFc-ALM form redox-sensitive ion channels. This work provides further evidence that CFPs can be rationally designed to posses unique properties and responses to chemical and electrical environment. In addition, these peptides are additions to the arsenal of tools that may be used to unravel the relationship between structure and function in CFPs and ion channels.

ACKNOWLEDGMENT

We thank Dr. Len Packman of the University of Cambridge for mass spectrographic analysis and John Kamial, Steve Dobson, Avtar Roopra, and Jenny Rodger for preliminary studies on this system.

REFERENCES

Acton, E. M., & Silverstein, R. M. (1959) *J. Org. Chem. 24*, 1487−1490.
Akerfeldt, K. S., Lear, J. D., Wasserman, Z. R., Chung, L. A., & DeGrado, W. F. (1993) *Acc. Chem. Res. 26*, 191−197.
Baumann, G., & Mueller, P. (1974) *J. Supramol. Struct. 2*, 538−557.
Boheim, G. (1974) *J. Membr. Biol. 19*, 277−303.
Boheim, G., Hanke, W., & Jung, G. (1983) *Biophys. Struct. Mech. 9*, 181−191.
Casico, M., & Wallace, B. A. (1988) *Proteins: Struct., Funct., Genet. 4*, 89−98.
Cornut, I., Buttner, K., Dasseux, J.-L., & Dufourcq, J. (1994) *FEBS Lett. 349*, 29−33.
DeGrado, W. F., & Lear, J. D. (1990) *Biopolymers 29*, 205−213.
Dougherty, D. A., & Stauffer, D. A. (1990) *Science 250*, 1558−1560.
Fox, R. O., & Richards, F. M. (1982) *Nature 350*, 325−330.
Ghadiri, M. R., Granja, J. R., Milligan, R. A., McRee, D. E., & Kazanovich, N. (1993) *Nature 366*, 324−327.
Ghadiri, M. R., Granja, J. R., & Buehler, L. K. (1994) *Nature 369*, 301−304.
Hall, J. E., Vodaynoy, I., Balasubramanian, T. M., & Marshall, G. M. (1984) *Biophys. J. 45*, 233−247.
Hanke, W., & Schule, W.-R. (1993) *Biological Techniques: Planar Lipid Bilayers*, Academic Press, London.
Karlin, A., & Akabas, M. H. (1995) *Neuron 15*, 1231−1244.
Latorre, R., & Alverez, O. (1981) *Physiol. Rev. 61*, 77−150.
Lau, H. H., & Hart, H. (1959) *J. Org. Chem. 24*, 280−281.
Montal, M., & Mueller, P. (1972) *Proc. Natl. Acad. Sci. U.S.A. 69*, 3561−3566.
Nesmeyanov, N., & Reutov, O. A. (1957) *Proc. Doc. Chem. 115*, 763−765.
Pearlman, R. S. (1980) *Physical Chemistry Properties of Drugs* (Yalkowsky, S. H., Sinkula, A. A., & Valvani, Y. C., Eds.) Dekker, New York.
Rappé, A. K., & Goddard, W. A. (1991) *J. Phys. Chem.* 95, 3358−3361.
Sansom, M. S. P. (1991) *Biophys. Mol. Biol. 55*, 139−236.
Sansom, M. S. P. (1993a) *Q. Rev. Biophys. 26*, 365−421.
Sansom, M. S. P. (1993b) *Eur. Biophys. J. 22*, 105−124.
Schnur, J. M., & Peckerar, M. (1992) *Synthetic Microstructures in Biological Research*, Plenum Press, New York.
Schwartz, G. (1987) *Biophys. Chem. 26*, 163−169.
Stankowski, S., & Schwartz, G. (1989) *FEBS Lett. 250*, 556−560.
Unwin, N. (1993) *Neuron 10 (Suppl.)*, 31−41.
Vogel, H. (1987) *Biochemistry 26*, 4562−4572.
Woolley, G. A., & Deber, C. M. (1993) *Biochemistry 32*, 9819−9825.
Woolley, G. A., & Wallace, B. A. (1993) *Biochemistry 32*, 9819−9825.
Woolley, G. A., Epand, R. M., Kerr, I. D., Sansom, M. S. P., & Wallace, B. A. (1994) *Biochemistry 33*, 6850−6858.
You, S., Peng, S., Lien, L., Breed, J., & Woolley, G. A. (1996) *Biochemistry 35*, 6225−6232.

BI962168W